Energy Engineering

Tech Science Press

DOI: 10.32604/ee.2022.017288

ARTICLE

Optimization Scheme of Integrated Community Energy Utilization System Based on Improved Sine-Cosine Algorithm

Xin Zhang*, Jinpeng Jiang, Haoran Zheng and Jihong Zhang

School of Information Engineering, Inner Mongolia University of Science & Technology, Baotou, 014010, China

*Corresponding Author: Xin Zhang. Email: zhangxin19861986@126.com

Received: 05 May 2021 Accepted: 02 July 2021

ABSTRACT

China consumes significant amount of natural gas in winter. The integrated community energy utilization system (ICEUS) cannot stabilize the output of electricity and heat if there is a shortage of natural gas. The operation cost of the system still needs improvement. An energy supply structure using garbage power as the core of ICEUS was established in the study. The optimal dispatching model of ICEUS was established using the regulating characteristic of the community load. The sine-cosine algorithm (SCA) based on nonlinear factors and segmented weight was presented to solve the optimal dispatching model of ICEUS. From the simulation results, compared with particle swarm optimization algorithm (PSO), SCA, exponential sine-cosine algorithm (ESCA), and parabolic sine-cosine algorithm (PSCA), the daily operation cost of ICEUS was reduced by the improved SCA by 4.4%, 2.9%, 2.6% and 4.1%, respectively, in winter. The same was true in summer. The daily system operating cost was effectively reduced by the algorithm proposed in the study. The cost benefits of the optimized ICEUS operation was realized.

KEYWORDS

Multi-energy; ICEUS; SCA; optimal dispatch; PSO

Nomenclature

Variables

P^t_{HWASTE}	Heat power of garbage power generation combined device
P^t_{CWASTE}	Cool power of garbage power generation combined device
P^t_{EWASTE}	Electrical power of garbage power generation combined device
η_{E}	Electrical transmission effectiveness of garbage power generation combined device
η_{H}	Heat transmission effectiveness of garbage power generation combined device
η_{C}	Cool transmission effectiveness of garbage power generation combined device
η_{re}	Recovery rate of flue gas waste heat
P^t_{CASHP}	Cool transmission power of the air source heat pump system
P^t_{HASHP}	Heat transmission power of the air source heat pump system
P^t_{ASHP}	Consumption power of the air source heat pump system
η_{HASHP}	Heat transmission effectiveness
η_{CASHP}	Cool transmission effectiveness

S^t_{stor}	Charged state of the lithium-ion battery storage and cool-heat storage device
δ	Self-discharge efficiency of the lithium-ion battery storage and cool-heat storage device
P^t_{ch}	Charging power for the lithium-ion battery storage and cool-heat storage device
P^t_{dis}	Discharging power of the lithium-ion battery storage and cool-heat storage device
η_{ch}	Charging efficiency of the lithium-ion battery storage and cool-heat storage device
η_{dis}	Discharging efficiency of the lithium-ion battery storage and cool-heat storage device
E_{tstor}	The total energy capacity of the lithium-ion battery storage and cool-heat storage device
e^t_{BUY}	The electricity buying price of the integrated community energy utilization system
e^t_{SELL}	The electricity selling price of the integrated community energy utilization system
P^t_{EX}	Electrical power transaction value between the integrated community energy utilization system and the distribution network
P^t_{WT}	Wind power
P^t_{PV}	Photovoltaic power
P^t_{ASHP}	Power consumption of the air source heat pump
P^t_{ESTOR}	Electrical power of the lithium-ion battery
P^t_{HSTOR}	Heat power of the heat energy storage device
P^t_{CSTOR}	Cool power of the cool energy storage device
C_{WT}	Maintenance cost of wind power generation
C_{PV}	Maintenance cost of photovoltaic generation
C_{WASTE}	Maintenance cost of the garbage power generation combined device
C_{ASHP}	Maintenance cost of the air source heat pump
C_{ESTOR}	Maintenance cost of the lithium-ion battery
C_{HSTOR}	Maintenance cost of the heat energy storage device
C_{CSTOR}	Maintenance cost of the cool energy storage device
$P^t_{electriload}$	Electrical load
$P^t_{heatload}$	Heat load
$P^t_{coolload}$	Cool load
X^t_{ij}	Position of the individual
r_1	Control parameter
P^t_{gj}	Global optimal solution to the population

Abbreviations

PSO	Particle swarm optimization
SCA	Sine-cosine algorithm
ESCA	Exponential sine-cosine algorithm
PSCA	Parabolic sine-cosine algorithm
PV	Photovoltaic
ICEUS	Integrated community energy utilization system

1 Introduction

With increasingly serious global environmental problems and continuous depletion of traditional fossil energy, renewable energy technology has become the focus of attention worldwide [1–3]. Therefore, the integrated energy network concept arises at this historic moment [4,5]. Energy supply networks (power grids, natural gas networks and cool-heat networks), energy exchange units (cool-heat-electricity supply units and air-source heat pumps), energy storage units (batteries and cold-heat storage devices) and a large number of integrated terminal energy units have been included in integrated energy networks. The multidirectional interaction of cool-heat-electricity-gas energy flow has been achieved. The sharing and stable renewable energy applications among multiple networks to meet the growing demand for high-quality energy services [6,7] have been implemented. The integrated energy unit configured in urban communities refers to ICEUS, the

integrated terminal energy utilization unit. With the accelerating urbanization process in China, areas of urban power grids and heating have expanded rapidly. However, there are some problems in communities of urban fringes, such as poor power quality and substandard heating temperatures. Through studying ICEUS, various renewable resources can be fully utilized to achieve a high-quality electricity-heat supply in the community. Given that the upgrading of distribution networks and heating units is delayed, ICEUS is of great guiding significance to the construction and development of urban communities in China.

At present, there have been domestic and international studies on the optimal dispatch of integrated energy networks [8–25]. Rural micro-energy grids are constructed, and the corresponding day-ahead optimal dispatch model of multienergy flow micro-energy grids is established. The optimal dispatching model on rural micro-energy grids is based on the improved hybrid PSO. The example analysis results show that the above algorithm can achieve the cost-effective operation of rural micro-energy grids in [8]. The optimal dispatching process of micro-energy grids is divided into two stages. A double-layer optimal dispatching model is established, and a micro-energy grid based on the model predictive control is used to make the optimal dispatching scheme of the micro-energy grid more accurate in [9]. The objective function for the lowest operating cost of micro-energy grids is constructed. A genetic algorithm based on a memory mechanism is proposed to solve the objective function in [10]. A hybrid PSO is proposed to optimize the cost-effective operation model of micro-energy grids in [11]. Cinar et al. [12] used SCA to solve the optimized management problem of a multienergy storage system. Pang et al. [13] proposed a multiunit coordinated operation strategy. SCA is used to formulate unit combinations. PSO, the genetic algorithm, and SCA are usually used to solve the optimal model in the above papers. However, these algorithms are relatively conventional, and the solution process can easily be stuck in a local optimization, making the realization of a globally optimal solution impossible. Tan et al. [14] designed an independent micro-energy grid structure of all renewable energy for islands or remote mountainous areas. The example verifies the feasibility, economy and reliability of the model. Zhang et al. [15] established the operation structure of a distribution network with micro-energy grids. A double-layer optimal model and an improved gray wolf optimal solving algorithm are proposed, and the coordinated distribution networks with micro-energy grids is achieved. Liu et al. [16] proposed energy management and optimization of a single micro-energy grid based on deep reinforcement learning. Hua et al. [17] established an energy internet model consisting of multimicro energy grids. The solution method is deep reinforcement learning. Li et al. [19] proposed an optimal dispatch method of island micro-energy grids, including the uncertainty of load and renewable energy. CPLEX solves the model to realize the optimal operation of island micro-energy grids. Considering the randomness of renewable energy and the comfortability for users, Li et al. [20] proposed an optimal dispatch model of the integrated energy utilization system based on chance-constrained programming. Zhang et al. [21] used the deep learning method to coordinate and optimize micro-energy grids' hybrid energy storage system. Li et al. [22] established a stochastic robust optimal operation model of a community-integrated energy system based on integrated demand response. Gao et al. [23] demonstrated a robust chance-constrained optimization model for the day-ahead economic dispatch of an integrated energy utilization system of electricity, gas and heat based on distributed robust optimization technology. Li et al. [24] established a two-stage optimal operation model of an integrated energy system. In [26], a multitime-space scale optimal operation strategy of the integrated energy system is proposed. In the above references, regulation of the user-side load has not been fully considered, and the economy and reliability of the system operation have further improved the space. In [27], the integrated energy system includes, new energy producer, integrated energy service producer, and

consumers. Considering multiagent interest balance and gas cost, the integrated energy system model is established. The improved NSGA-II is used to solve the model. In [28], natural gas was used as the fuel input for the cold-heat-electricity supply unit. An optimal dispatch method of the integrated energy utilization system is proposed based on a Stackelberg game. In [29], the deployment of island microgrids was studied. Natural gas is also a major energy source. However, China has a high consumption of natural gas, especially in winter. The shortage of natural gas may cause the failure of ICEUS to output stable electricity and heat, which brings enormous losses to users.

In conclusion, there are still the following problems in the optimal dispatch of ICEUS:

1) There are usually PSO, the genetic algorithm and SCA in solving the optimal model in the existing references. These algorithms are relatively conventional, and the solution process is easily stuck in a local optimum, making the global optimal solution impossible. The cost-effective operation of ICEUS has not been achieved.
2) Some of the above references have not fully considered the regulation of the user-side load. Introducing the regulation technology of the user-side load into ICEUS can effectively guarantee the real-time balance of energy in the network and improve system operation's economy and reliability.
3) The consumption of natural gas in winter is high in China. Taking natural gas as the fuel input for cold-heat-electricity supply units may cause problems in the above references. Due to the shortage of natural gas, electricity-heat energy cannot be stably output in ICEUS.

This study aims to solve the above problems, and its contributions are as follows:

1) Garbage power was proposed as a thermoelectric coupling device that did not consume natural gas. At the same time, urban garbage could be consumed effectively.
2) The energy supply structure of ICEUS was established, which included a distributed wind power, photovoltaic (PV) power and garbage power generation combined system, air-source heat pump, lithium-ion storage device and cold-heat storage device.
3) Considering the regulation of the user-side load, the optimal dispatch model of ICEUS was constructed.
4) An improved SCA based on nonlinear factors and segmented weights was proposed to solve the dispatching model. SCA was superior to PSO and genetic algorithms in operation speed, global search ability and convergence accuracy. The improved SCA based on nonlinear factors and segmented weight provided a strong algorithm guarantee for the optimal operation of ICEUS.

The organizational structure of the study is as follows. Section 2 establishes the energy supply structure of ICEUS and sets the mathematical model of energy supply and energy storage devices. The optimal dispatch model of ICEUS is built. In Section 3, the improved SCA based on nonlinear factors and segmented weight was proposed, and the algorithm's effectiveness was verified. An example was used to verify the model and method presented in Section 4. In Section 5, the entire paper is summarized, and future research work is explored. The general workflow of the study is shown in Fig. 1.

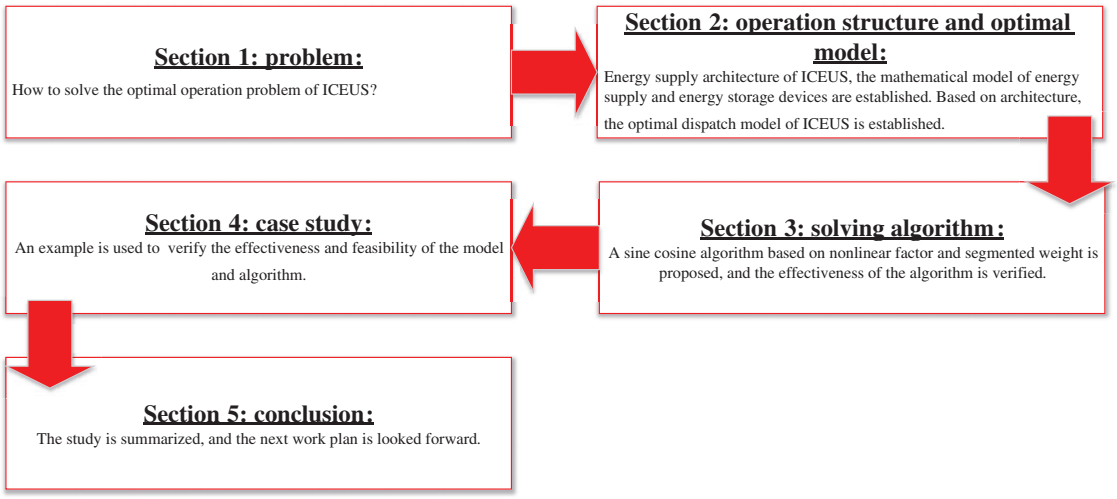

Figure 1: General workflow of the study

2 The Structure of ICEUS

ICEUS was mainly composed of energy production, transmission, conversion, storage, and utilization units. The cold-heat-electricity-gas energy flow could achieve multiway interaction and mutual support through energy conversion devices, power grids and cold-heat pipe networks. By doing so, the integrated and efficient utilization of a variety of energy sources was achieved. The system structure is shown in Fig. 2.

1) The energy production unit was a device that converted wind, solar and natural gas power into cold-heat-electricity energy required by the system. The unit mainly included a distributed wind power, PV power and garbage power generation combined system.
2) The energy transmission unit referred to the transmission channel between various types of energy and load points, and it mainly included the power grid and the cold-heat energy network.
3) The energy conversion unit refers to the energy converting device of cool-heat-electricity-gas. It includes the air-source heat pump, the lithium-bromide absorption-type refrigerator and the heat recovery boiler.
4) The energy storage unit referred to the power storage device of cool-heat-electricity, and it included the lithium-ion battery and the power storage device of cool-heat-electricity. The main role of the energy storage unit was to smooth the power fluctuations of renewable energy sources such as wind power and PV power and to realize the function of peak cutting and valley filling in the system.
5) The energy utilization unit refers to the cool-heat-electricity load point in the system.

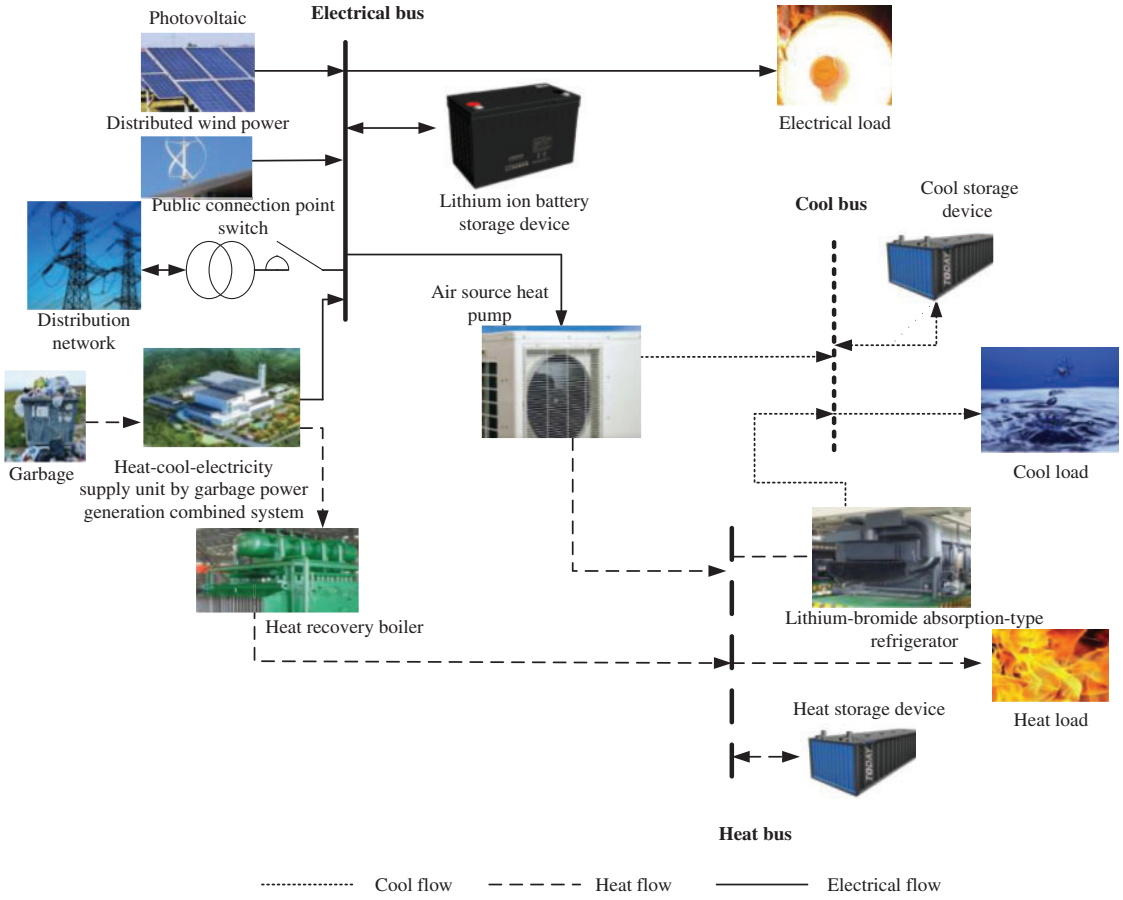

Figure 2: Structure of ICEUS

2.1 Mathematical Model of Garbage Power Generation Combined System

The garbage power generation combined system mainly included garbage generators, heat recovery boilers, and lithium-bromide absorption-type refrigerators. The integrated garbage power generation system used crushed garbage powder to drive garbage generators to generate electricity. The high-temperature flue gas produced in combustion generates heat energy through the heat recovery boiler to meet the heat load demand of community residents in winter. The high-temperature steam produced by the heat recovery boiler generated cooling power through the lithium-bromide absorption-type refrigerator to meet the cooling load demand of community residents in summer. The mathematical model is defined as follows:

$$P^t_{\mathrm{HWASTE}} = \frac{P^t_{\mathrm{EWASTE}}(1-\eta_{\mathrm{E}})}{\eta_{\mathrm{E}}}\eta_{\mathrm{H}}\eta_{\mathrm{re}} \tag{1}$$

$$P^t_{\mathrm{CWASTE}} = \frac{P^t_{\mathrm{EWASTE}}(1-\eta_{\mathrm{E}})}{\eta_{\mathrm{E}}}\eta_{\mathrm{H}}\eta_{\mathrm{re}}\eta_{\mathrm{C}} \tag{2}$$

where P^t_{HWASTE} is the heat power of the combined system, P^t_{CWASTE} is the cooling power, P^t_{EWASTE} is the electrical power of the integrated system, η_{E} is the electricity transmission

effectiveness, η_H is the heat transmission effectiveness of the integrated system, η_C is the cool transmission effectiveness, and η_{re} is the recovery rate of flue gas waste heat.

2.2 Mathematical Model of Air Source Heat Pump

The air-source heat pump was a device that drove working fluid circulation through a compressor fueled by electricity. It could convert low heat energy to the required high heat energy and have a cooling function. The mathematical model is defined as follows:

$$P^t_{HASHP} = \eta_{HASHP} P^t_{ASHP} \tag{3}$$

$$P^t_{CASHP} = \eta_{CASHP} P^t_{ASHP} \tag{4}$$

where P^t_{CASHP} is the cool transmission power, P^t_{HASHP} is the heat transmission power, P^t_{ASHP} is the consumption power, η_{HASHP} is the heat transmission effectiveness, and η_{CASHP} is the cool transmission effectiveness.

2.3 Mathematical Model of Lithium-Ion Battery Storage and Cool-Heat Storage Device

The charging and discharging principles of lithium-ion battery storage and cool-heat storage devices were similar. The related model is as follows:

$$S^t_{stor} = S^{t-1}_{stor}(1-\delta) + \Delta T P^t_{ch}\eta_{ch}/E_{tstor} - \Delta T P^t_{dis}/(\eta_{dis}E_{tstor}) \tag{5}$$

where S^t_{stor} is the charged state of the lithium-ion battery storage and cool-heat storage device, δ is the self-discharge efficiency of the device, P^t_{ch} is the charging power of the device, P^t_{dis} is the discharging power, η_{ch} is the charging efficiency of the device, η_{dis} is the discharging efficiency, and E_{tstor} is the total energy capacity of the lithium-ion battery storage and cool-heat storage device.

2.4 Objective Function of the Optimal Dispatching Model on ICEUS

The optimal dispatching objective function of ICEUS constructed in this study had the lowest daily system operating cost. The raw material for the garbage power plant was domestic garbage, which was provided free by users in the service zones of ICEUS, and there was an adequate supply of domestic garbage. Daily operation costs of ICEUS included the electricity transaction cost with the distribution network and the maintenance cost of the system's energy supply and storage devices. The objective function is as follows:

$$\begin{aligned}\min C = \sum_{t=1}^{24} \Bigg(& \frac{e^t_{BUY} + e^t_{SELL}}{2} P^t_{EX} + \frac{e^t_{BUY} - e^t_{SELL}}{2} |P^t_{EX}| + C_{WT} P^t_{WT} + C_{PV} P^t_{PV} + C_{WSATE} P^t_{EWASTE} \\ & + C_{WSATE} P^t_{HWASTE} + C_{ASHP} P^t_{ASHP} + C_{ESTOR} |P^t_{ESTOR}| + C_{HSTOR} |P^t_{HSTOR}| \\ & + C_{CSTOR} |P^t_{CSTOR}| \Bigg)\end{aligned} \tag{6}$$

where e^t_{BUY} is the electricity buying price of ICEUS and e^t_{SELL} is the electricity selling price of the system; P^t_{EX} is the electricity transaction value between ICEUS and the distribution network (electricity buying value is positive and electricity selling value is negative); P^t_{WT} is wind power; P^t_{PV} is PV power; P^t_{ASHP} is the power consumption of the air-source heat pump; P^t_{ESTOR} is the electrical power of the lithium-ion battery (discharging power value is positive and charging power value is negative); P^t_{HSTOR} is the heat power of the heat energy storage device (discharging heat

power value is positive and charging heat power value is negative); P^t_{CSTOR} is the cooling power of cooling power storage device (discharging cooling power value is positive and charging cooling power value is negative); C_{WT} is the maintenance cost of wind power generation; C_{PV} is the maintenance cost of PV power generation; C_{WASTE} is the maintenance cost of the garbage power generation combined device; C_{ASHP} is the maintenance cost of the air-source heat pump; C_{ESTOR} is the maintenance cost of the PV power generation; C_{HSTOR} is the maintenance cost of C_{CSTOR} is the maintenance cost of the garbage power storage device.

2.5 Constraints of the Optimal Dispatching Model on ICEUS

1) Constraint condition of electrical power balance

$$P^t_{\mathrm{ESTOR}} + P^t_{\mathrm{EWASTE}} + P^t_{\mathrm{EX}} + P^t_{\mathrm{WT}} + P^t_{\mathrm{PV}} - P^{\mathrm{t}}_{\mathrm{ASHP}} = P^t_{\mathrm{electriload}} \tag{7}$$

where $P^t_{\mathrm{electriload}}$ is the electrical load.

2) Constraint condition of heat power balance

$$P^t_{\mathrm{HASHP}} + P^t_{\mathrm{HWASTE}} + P^t_{\mathrm{HSTOR}} = P^t_{\mathrm{heatload}} \tag{8}$$

where P^t_{heatload} is the heat load.

3) Constraint condition of cooling power balance

$$P^t_{\mathrm{CASHP}} + P^t_{\mathrm{CWASTE}} + P^t_{\mathrm{CSTOR}} = P^t_{\mathrm{coolload}} \tag{9}$$

where, P^t_{coolload} is the cooling load.

4) Constraint condition of the garbage power generation combined device

$$P^{\min}_{\mathrm{EWASTE}} \le P^t_{\mathrm{EWASTE}} \le P^{\max}_{\mathrm{EWASTE}} \tag{10}$$

where $P^{\min}_{\mathrm{EWASTE}}$ and $P^{\max}_{\mathrm{EWASTE}}$ are the minimum and maximum power output of the garbage power generation combined device, respectively.

5) Constraint condition of the lithium-ion battery storage and cool-heat storage device

Because the function and principle of the lithium-ion battery storage and cool-heat storage device were similar, the general model can be used as the constraint condition.

$$S^{\min}_{\mathrm{stor}} \le S^t_{\mathrm{stor}} \le S^{\max}_{\mathrm{stor}} \tag{11}$$

$$S^0_{\mathrm{stor}} = S^T_{\mathrm{stor}} \tag{12}$$

$$0 \le P^t_{\mathrm{dis}} \le P_{\mathrm{dmax}} \tag{13}$$

$$0 \le P^t_{\mathrm{ch}} \le P_{\mathrm{cmax}} \tag{14}$$

$$P^t_{\mathrm{stor}} = \begin{cases} P^t_{\mathrm{dis}}, P^t_{\mathrm{stor}} \ge 0 \\ -P^t_{\mathrm{ch}}, P^t_{\mathrm{stor}} < 0 \end{cases} \tag{15}$$

where $S^{\max}_{\mathrm{stor}}$ and $S^{\min}_{\mathrm{stor}}$ are the maximum and minimum charged states of the lithium-ion battery storage and cool-heat storage device, respectively; P_{cmax} and P_{dmax} are the maximum charging

power and maximum discharging power of the device, respectively; and P^t_{stor} is the charging and discharging power of the device.

6) Constraint condition of the air-source heat pump

$$0 \le P^t_{\text{ASHP}} \le P^{\max}_{\text{ASHP}} \tag{16}$$

where $P^{\max}_{\text{HASHP}}$ is the maximum power consumption of the air-source heat pump.

7) Constraint condition of reserve power

$$P^{\max}_{\text{WT}} + P^{\max}_{\text{PV}} + P^{\max}_{\text{EWASTE}} + P^{\max}_{\text{EX}} \ge P^t_{\text{electriload}}(1 + Y_{\text{res}}) \tag{17}$$

where $P^{\max}_{\text{WT}}$ is the maximum power of wind power generation; $P^{\max}_{\text{PV}}$ is the maximum power of PV power generation; $P^{\max}_{\text{EX}}$ is the maximum power transaction between ICEUS and the external distribution network; and Y_{res} is the system reserve rate.

8) Constraint condition of the power transaction between ICEUS and the external distribution network

$$P^{\min}_{\text{EX}} \le P^t_{\text{EX}} \le P^{\max}_{\text{EX}} \tag{18}$$

where $P^{\min}_{\text{EX}}$ is minimum power transaction between ICEUS and the external distribution network.

9) Constraint condition of regulating load

The electricity load was divided into the regulating load and the nonregulating load in the study. The regulating load indicated that the electricity supply time of the load could be changed. The nonregulating load suggested that the electricity supply time of the load could not be changed. The relevant constraints are as follows:

$$P_{\text{after}}(t) = P_{\text{fore}}(t) + \sum_{k=1}^{s} P_k(t', t) + \sum_{k=1}^{s} P_k(t, t'') \tag{19}$$

$$\sum_{t=1}^{T} P_{\text{after}}(t) = \sum_{t=1}^{T} P_{\text{fore}}(t) \tag{20}$$

where $P_{\text{fore}}(t)$ and $P_{\text{after}}(t)$ are the power values before and after the load regulation, respectively; $P_k(t, t'')$ and $P_k(t', t)$ are the power transmission values of the class k load.

3 Solution to the Optimal Dispatching Model on ICEUS

3.1 Improved SCA Based on Nonlinear Factors and Segment Weight

The optimal dispatch model of ICEUS established in this study had a multivariate nonlinear optimization problem with complex equations. Therefore, an improved SCA based on nonlinear factors and segment weight was proposed to solve the optimal model. SCA [30] was proposed by Australian scholar in 2015. In the algorithm, the individual state update was achieved by changing the mathematical functions of Sine and Cosine. SCA kept the population diversity early, maintained a strong search ability and strengthened the individual local development ability in the

later stage. Finally, the global optimal solution was obtained. Formulas included in the algorithm are as follows:

$$X_{ij}^{t}=\begin{cases} d_{\text{weight}}^{t}\times X_{ij}^{t}+r_1\times\sin(r_2)\times|r_3P_{gj}^{t}-X_{ij}^{t}|, & r_4<0.5 \\ d_{\text{weight}}^{t}\times X_{ij}^{t}+r_1\times\sin(r_2)\times|r_3P_{gj}^{t}-X_{ij}^{t}|, & r_4\geq 0.5 \end{cases} \tag{21}$$

$$r_1=a-t\frac{a}{T} \tag{22}$$

where formula (21) is the individual update formula in the algorithm; X_{ij}^{t} is the position of the individual i in the space j at iteration t; r_1 is the control parameter; P_{gj}^{t} is the global optimal solution to the population; r_2, r_3 and r_4 are random numbers, and the ranges are $r_2\in[0,2\pi]$, $r_3\in[-2,2]$, and $r_4\in[-1,1]$, respectively; $a=2$; and T is the maximum iteration number.

Concerning the problem that the traditional sine-cosine algorithm is easily stuck in a local optimum and has poor convergence accuracy, the following improvement schemes were proposed in the study:

1) The control parameter r_1 was changed from a linear function to a nonlinear function, which was more suitable for the algorithm's actual search process and enhanced the algorithm's search ability. The improved formula is as follows:

$$r_1=\sqrt{1-\left(\frac{t}{T}\right)^2} \tag{23}$$

2) The updating formula (21) of the individual position was improved. The weight factor was increased. The improved results enabled the algorithm to break out of the trap of local minima more easily and improve the global search ability and convergence accuracy. The improved formulas are as follows:

$$d_{\text{weight}}^{t}=\begin{cases} 1-\frac{t}{T}+e^{(-r_1-r_2-2)}, & t<\frac{T}{2} \\ 1-0.9^{(\frac{t}{T})}, & t>\frac{T}{2} \end{cases} \tag{24}$$

$$X_{ij}^{t}=\begin{cases} d_{\text{weight}}^{t}\times X_{ij}^{t}+r_1\times\sin(r_2)\times|r_3P_{gj}^{t}-X_{ij}^{t}|, & r_4<0.5 \\ d_{\text{weight}}^{t}\times X_{ij}^{t}+r_1\times\sin(r_2)\times|r_3P_{gj}^{t}-X_{ij}^{t}|, & r_4\geq 0.5 \end{cases} \tag{25}$$

where d_{weight}^{t} is the weight factor.

Each individual in the sine-cosine algorithm represents a solution. The solving steps of the dispatch model of ICEUS by the improved SCA were as follows.

1) Population initialization

The parameters of energy supply devices in ICEUS were randomly initialized as a set of solutions in the range values of energy supply devices.

2) The fitness of each individual was calculated, and the optimal individual position was found.

Using the improved sine-cosine algorithm, the objective function formula (6) was solved. A set of optimal solutions for energy supply devices of the integrated community energy were obtained.

3) The individual position was updated based on formulas (23–25)

Formulas (23–25) were used to update a set of solutions to energy supply devices. Then the objective function formula (6) was recalculated to determine whether the current objective function value was better than the previous objective function value. If so, a set of solutions to the energy supply devices with the current objective function values were taken as the current global optimal solution.

4) If the current iteration number t was smaller than the maximum iteration number T, Step 3 was returned. Conversely, the algorithm ended and the final results were outputted.

The improved SCA was used to solve the dispatching model of ICEUS. The flow chart is shown in Fig. 3.

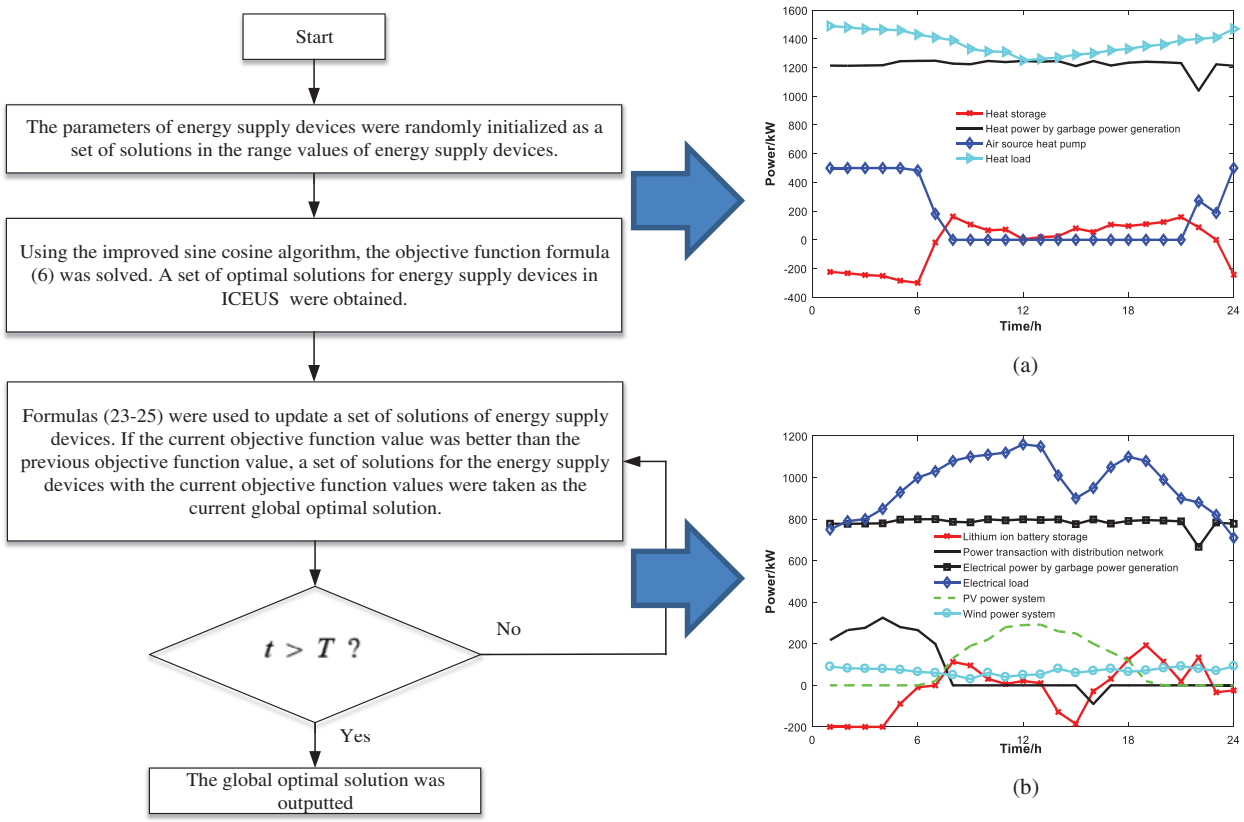

Figure 3: Flow chart of the dispatching model for ICEUS with improved sine-cosine algorithm. (a) Daily dispatching curve of the heat supply device in winter after electrical load regulation. (b) Daily dispatching curve of the electricity supply device in winter after electrical load regulation

3.2 Feasibility of Improved SCA

The six test functions were used to verify the feasibility of the algorithm proposed in the study. The six text functions were divided into two groups. One set of functions was a single-peak function including $f_1(x)$, $f_2(x)$, and $f_3(x)$. Another set was a multipeak function including $f_4(x)$, $f_5(x)$, and $f_6(x)$. Single-peak functions were used to test the global convergence of the algorithm. Multipeak functions were used to test the local convergence of the algorithm. The test function dimension was set to 10. The six test functions are shown in Table 1.

Table 1: Test functions

Test function	Search scope
$f_1(x) = \sum_{i=1}^{n} \lvert x_i \rvert + \prod_{i=1}^{n} \lvert x_i \rvert$	[−10, 10]
$f_2(x) = \sum_{i=1}^{n} i x_i^4 + random[0, 1]$	[−1.28, 1.28]
$f_3(x) = \sum_{i=1}^{n} x_i^2$	[−100, 100]
$f_4(x) = \sum_{i=1}^{n} [x_i^2 - 10\cos(2\pi x_i) + 10]$	[−5.12, 5.12]
$f_5(x) = -20\exp(-0.2\sqrt{\frac{1}{n}\sum_{i=1}^{n} x_i^2}) - \exp(\frac{1}{n}\sum_{i=1}^{n}\cos(2\pi x_i)) + 20 + e$	[−32, 32]
$0f_6(x) = \frac{1}{4000}\sum_{i=1}^{n} x_i^2 - \prod\cos(x_i/\sqrt{i}) + 1$	[−600, 600]

PSO [29], SCA [30], PSCA [31], ESCA [31], and the improved SCA proposed in the study were tested. The parameters of the PSO algorithm were as follows: the proportional weight was 0.8; the particle swarm size was 100; the learning factor was 2, and the maximum number of iterations was 200. The parameters of the SCA and its improved algorithm were as follows: the population size was 100, and the maximum number of iterations was 200. The above five algorithms were used to solve the test function, and the simulations are shown in Fig. 4.

Fig. 4 shows that compared with PSO, SCA, ESCA and PSCA, the improved SCA proposed in the study showed significant advantages in optimization ability and convergence speed in the optimal process of the five functions. For example, Function 6 was a multimodal function with more local minimum values. The improved SCA proposed in this paper was able to find the global optimal solution in iteration number 140. The optimal process efficiency of the improved SCA was higher than that of the other four algorithms, which proved the correctness and superiority of the proposed algorithm in this study.

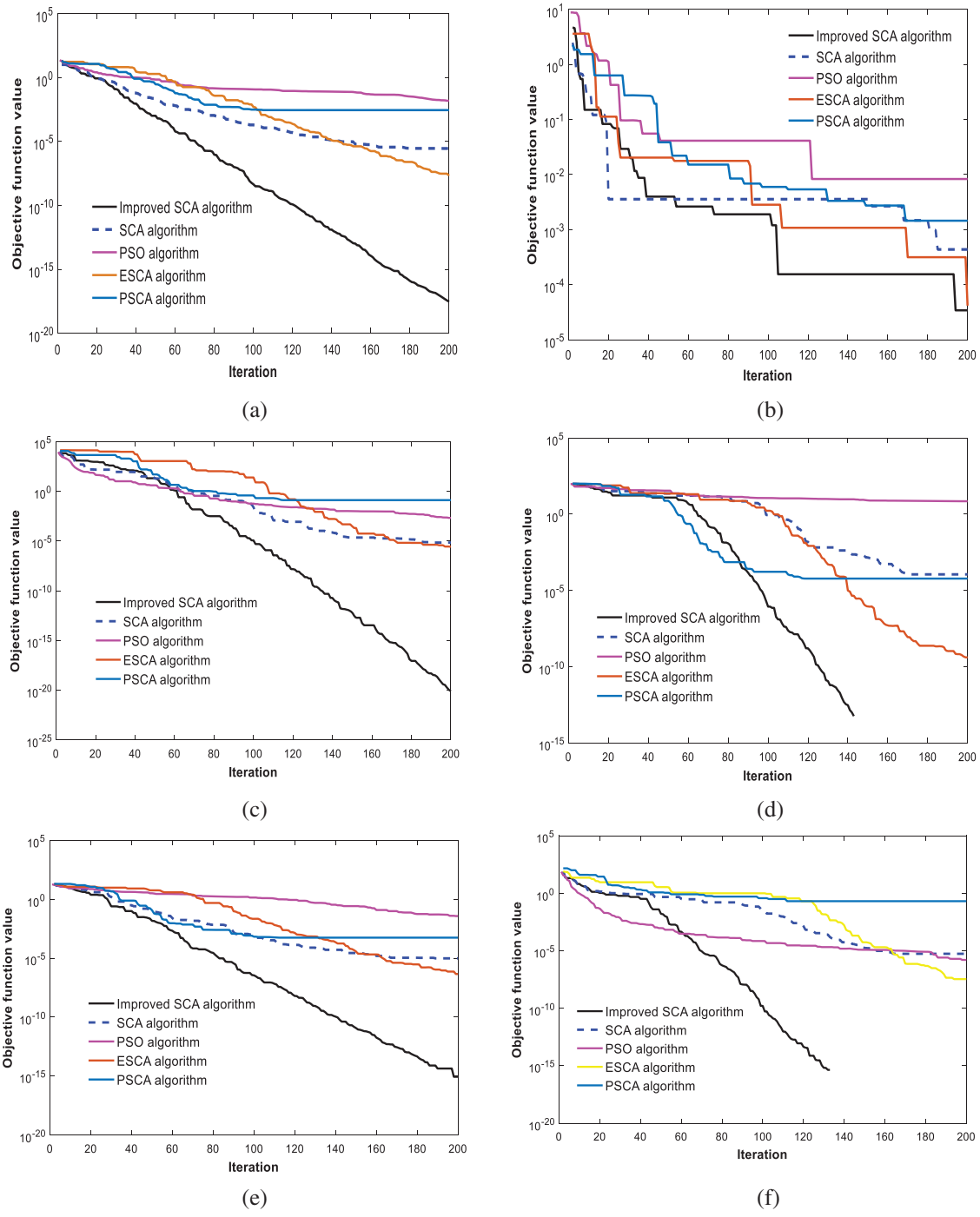

Figure 4: Effect comparison chart of the sine-cosine algorithm and its improved algorithm. (a) Function 1; (b) Function 2; (c) Function 3; (d) Function 4; (e) Function 5 (f) Function 6

4 Example Analysis

4.1 Basic Data

A city community in Western China was taken as a sample of the study. The electrical buying and selling prices of the power grid [32] are shown in Fig. 5. The daily heat-electricity load curves and wind power and PV power prediction curves in winter are shown in Fig. 6. The daily cool-electricity load curves and wind power and PV power prediction curves in summer are shown in Fig. 7. The curves in Figs. 6 and 7 were simulated by Monte Carlo technology [33,34]. The regulating characteristics of ICEUS are shown in Table 2. The parameters of energy supply devices in ICEUS are shown in Tables 3 and 4 [35–37]. The parameters of PSO were as follows: the proportional weight was 0.8; the particle swarm size was 100; the learning factor was 2; and the maximum number of iterations was 200. The parameters of the SCA and its improved algorithm were as follows: the population size was 100, and the maximum number of iterations was 200.

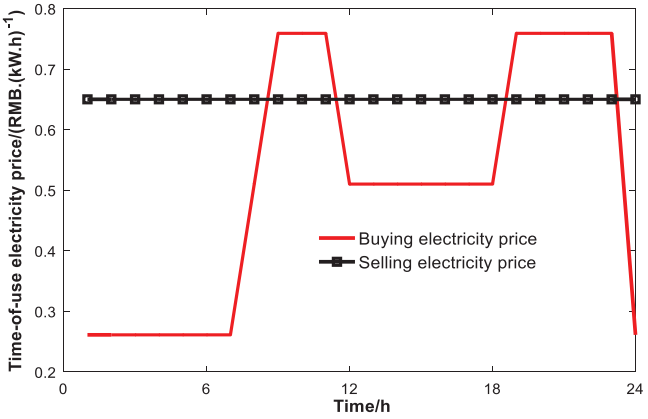

Figure 5: Electrical buying and selling prices of the power grid

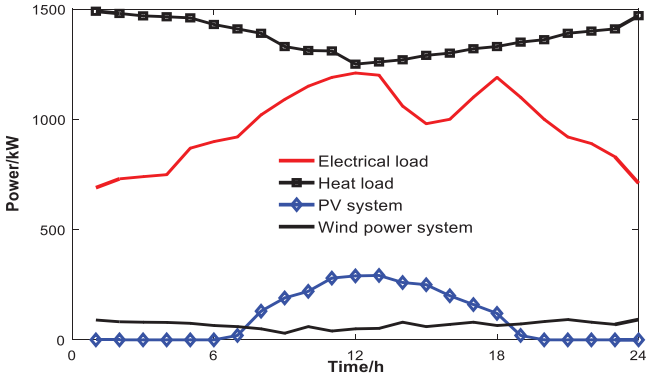

Figure 6: Daily heat-electricity load curves and wind power and PV power prediction curves in winter

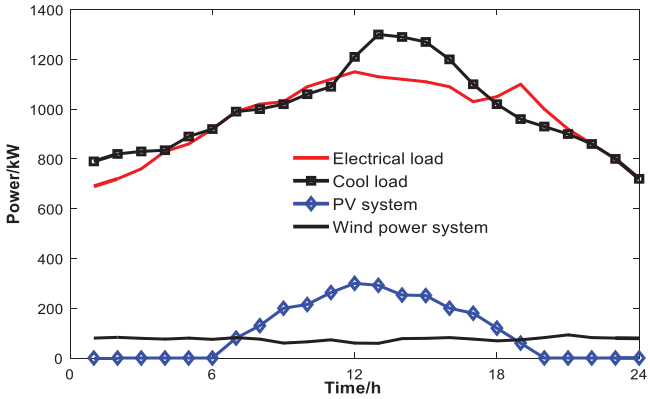

Figure 7: Daily cool-electricity load curves and wind power and PV power prediction curves in summer

Table 2: Regulating characteristics of the loads in ICEUS

Load	Regulating characteristic
Air conditioning	00:00–11:00, 14:30–18:00, regulation
Electric vehicle	00:00–24:00, regulation

Table 3: Parameters of the energy supply devices

Device	Parameter	Value
Garbage power generation combined system	Maximum generated power/kW	800
	Power generation efficiency	0.22
	Heat exchange efficiency	0.8
	Cool exchange efficiency	1.2
	Maintenance cost/RMB·(kW·h)$^{-1}$	0.02
Air source heat pump	Maximum heat and cool exchange power	500
	Heat and cool exchange efficiency	3.7
	Maintenance cost/RMB·(kW·h)$^{-1}$	0.03

(Continued)

Table 3 (Continued)

Device	Parameter	Value
Electrical power transaction with external distribution network	Maximum power/kW	1000
PV power generation	Maximum power/kW	300
	Maintenance cost/RMB·(kW·h)$^{-1}$	0.08
Wind power generation	Maximum power/kW	100
	Maintenance cost/RMB·(kW·h)$^{-1}$	0.11

Table 4: Parameters of the lithium-ion storage device and the cold-heat storage device

Device	Electricity/heat efficiency		Self-discharge electricity/heat efficiency	Electricity-charged and heat-charged state		Capacity/(kW·h)
	Maximum charge	Maximum charge		Maximum	Minimum	
Lithium-ion storage device	0.2	0.2	0.02	0.9	0.2	1000
Heat storage device	0.2	0.2	0.03	0.9	0.1	1500
Cool storage device	0.2	0.2	0.03	0.9	0.1	1500

According to the regulating characteristics of the loads in ICEUS at Table 2, related regulating load constraints, and electrical load model in reference [38], when loads transferred in or out were not allowed to reach 110 kW during each period, the internal point method would be used to obtain the winter typical electrical load curves before and after electrical load regulation in Fig. 8. The summer typical electrical load curves before and after electrical load regulation are shown in Fig. 9.

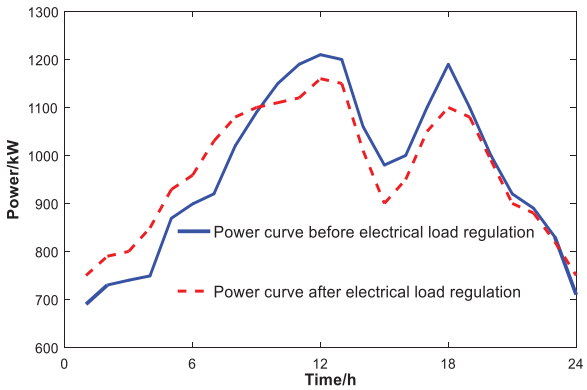

Figure 8: Daily electrical load power curves before and after electrical load regulation in winter

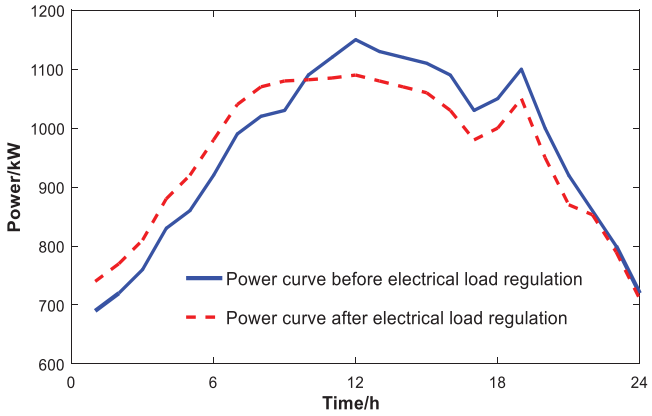

Figure 9: Daily electrical load power curves before and after electrical load regulation in summer

4.2 Daily Dispatching Curve of ICEUS before and after Electrical Load Regulation in Winter and Summer

Fig. 10 shows the daily dispatching curve of the heat supply device in winter before and after electrical load regulation. From Fig. 10, during low electricity price periods, i.e., 23:00–24:00 and 00:00–07:00, the air-source heat pump and the garbage power generation combined system could meet the heat load. The heat storage device was charged simultaneously. The integrated garbage power generation system became the main heat supply unit during the high electricity price period, i.e., 07:00–23:00. The unmet heat demand was satisfied by the heat storage device. The heat storage device was charged during the low electricity price period and discharged during the high electricity price period, which met the system demand. The output power was relatively stable because the integrated garbage power generation system was less affected by the electrical load regulation. The dispatching curves of the heat supply device were unchanged before and after electrical load regulation.

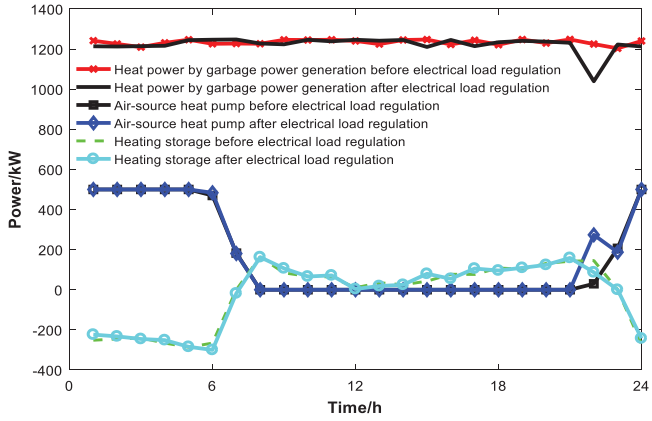

Figure 10: Daily dispatching curve of the heat supply device in winter before and after electrical load regulation

Fig. 11 shows the daily dispatching curve of the electricity supply device in winter before and after electrical load regulation. From Fig. 11, the common points are shown as follows before

and after electrical load regulation. During low electricity price periods, i.e., 23:00–24:00 and 00:00–07:00, the electricity load demands were satisfied by buying electricity from the distribution network, the garbage power generation combined system, and the wind power generation system. The lithium-ion battery was charged simultaneously. During the high electricity price period, i.e., 07:00–23:00, the buying price of electricity from external distribution networks was higher. The garbage power generation combined system, PV, wind, and lithium-ion batteries became the main electricity supply units. The function of the lithium-ion battery was peak cutting and valley filling. The different points are shown as follows before and after the electricity load regulation. During the flat and peak periods of the electricity price, except for the electricity required by the residents, the rest of the electricity could be connected to the external distribution network to gain revenues. In the valley period of the electricity price, a large amount of cheap electricity from the external distribution network was used to meet the electrical load demand.

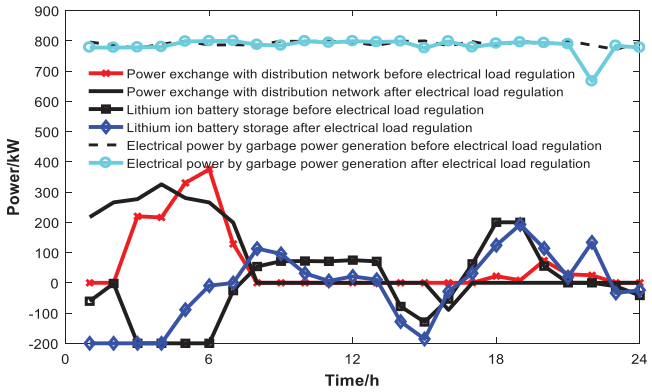

Figure 11: Daily dispatching curve of the electricity supply device in winter before and after electrical load regulation

Fig. 12 shows the daily dispatching curve of the cool supply device in the summer before and after electrical load regulation. Similar to the dispatching curve of the heat supply device in winter, during low electricity price periods, i.e., 23:00–24:00 and 00:00–07:00, the garbage power generation combined system met the cooling load. The excess cool power was stored in the cold storage device. The integrated garbage power generation system became the main cold supply unit during the high electricity price period, i.e., 07:00–23:00. The unmet cold demand was satisfied by the cool storage device and the air-source heat pump. The cool storage device was charged during the low electricity price period and discharged during the high electricity price period, which met the system demand. The output power was relatively stable because the integrated garbage power generation system was less affected by the electrical load regulation. The dispatching curve of the cold supply device was unchanged before and after electrical load regulation.

Fig. 13 shows the daily dispatching curve of the electricity supply device in the summer before and after electrical load regulation. Similar to the dispatching curve of the electricity supply device in winter, the common points are shown as follows before and after electrical load regulation. During low electricity price periods, i.e., 23:00–24:00 and 00:00–07:00, the electricity load demand was satisfied by purchasing electricity power from the distribution network, the garbage power generation combined system, and the wind power generation system. The lithium-ion battery was charged simultaneously. During the high electricity price period, i.e.,

07:00–23:00, the purchasing price of electricity from the external distribution network was higher. The integrated garbage power generation system, PV, wind, and lithium-ion batteries became the main electricity supply units. The function of the lithium-ion battery was peak cutting and valley filling. The differences are shown below before and after electrical load regulation. During the flat and peak periods of the electricity price, except for the electricity required for the residents, the rest of the electricity power could be connected to the external distribution network to gain revenues.

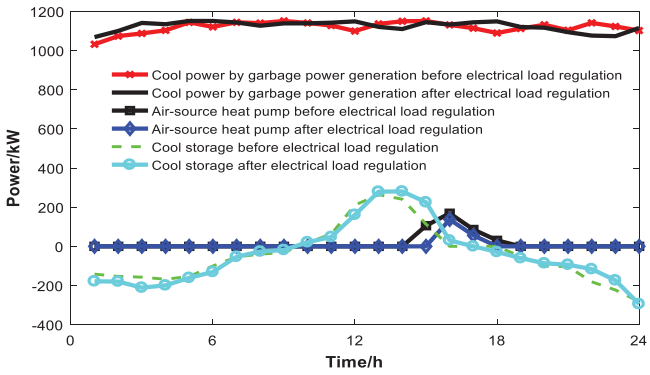

Figure 12: Daily dispatching curve of the cool supply device in summer before and after electrical load regulation

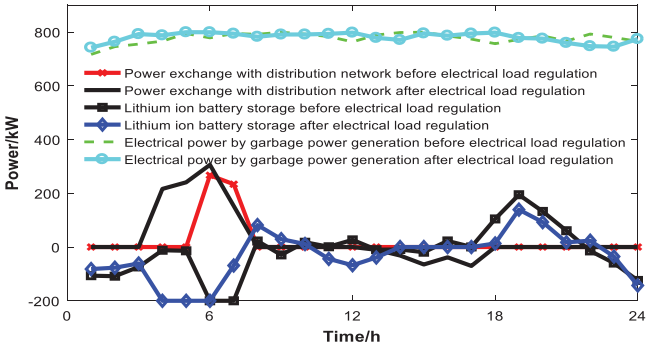

Figure 13: Daily dispatching curve of the electricity supply device in summer before and after electrical load regulation

4.3 Comparison of Daily Operating Costs of ICEUS before and after Electrical Load Regulation

Table 5 shows a comparison of the daily operating costs of ICEUS before and after electrical load regulation. Before the electrical load regulation, the daily operating cost of ICEUS was ¥2194.1 and ¥1707.1 in winter and summer, respectively. After the electrical load regulation, the daily operating cost of the system was ¥2165.9 and ¥1681.9 in winter and summer, respectively. The daily operating cost of the system was cut by 1.3% and 1.5% in winter and summer, respectively. It was proven that finding and controlling the regulating characteristics of the electrical load could reduce the daily operating costs of ICEUS. The economically feasible operation of the system was achieved.

Table 5: Comparison of daily operating cost of ICEUS before and after electrical load regulation

Season	Daily operating cost (¥)		Cost decline rate
	Before the electricity load is regulated	After the electricity load is regulated	
Winter	2194.1	2165.9	1.3%↓
Summer	1707.1	1681.9	1.5%↓

4.4 Performance Validity of the Improved SCA Proposed in the Study

The validity of the proposed algorithm in the paper was verified by PV power, wind power, and electricity-heat-cool load data on a typical day in both winter and summer after electrical load regulation. Fig. 14 shows the comparison curve of the daily operating cost of ICEUS based on five algorithms on a typical day in winter. The daily operating cost of ICEUS was ¥2265.6 by PSO [29], ¥2231.3 by SCA [30], ¥2224.3 by ESCA [31], and ¥2258.4 by PSCA [31]. Compared with PSO, SCA, ESCA, and PSCA, the daily operation cost of ICEUS by the improved SCA was reduced by 4.4%, 2.9%, 2.6% and 4.1%, respectively. The above results showed that a better global optimal solution could be found with the improved SCA, and a more economical daily operating cost and better device dispatching scheme could be obtained. Therefore, the validity and feasibility of the algorithm proposed in this paper was proven.

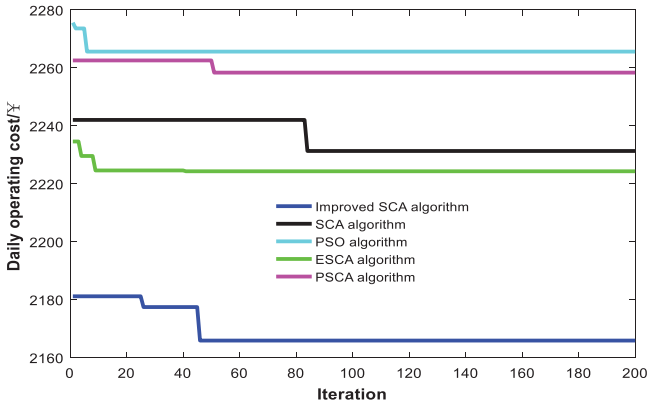

Figure 14: Comparison curve of the daily operating cost of ICEUS based on five algorithms on a typical day in winter

Fig. 15 shows the comparison curve of the daily operating cost of ICEUS based on five algorithms on a typical day in summer. The daily operating cost of the system was ¥2171.4 by PSO, ¥1733.9 by SCA, ¥1714.1 by ESCA, and ¥1757.4 by PSCA. Compared with PSO, SCA, ESCA and PSCA, the daily operation cost of ICEUS by the improved SCA was reduced by 22.5%, 3.0%, 1.9% and 4.3%, respectively. The above results showed that a better global optimal solution could be found with the improved SCA, and a more economical daily operating cost and better device dispatching scheme could be obtained. Therefore, the validity and feasibility of the algorithm proposed in this paper was proven.

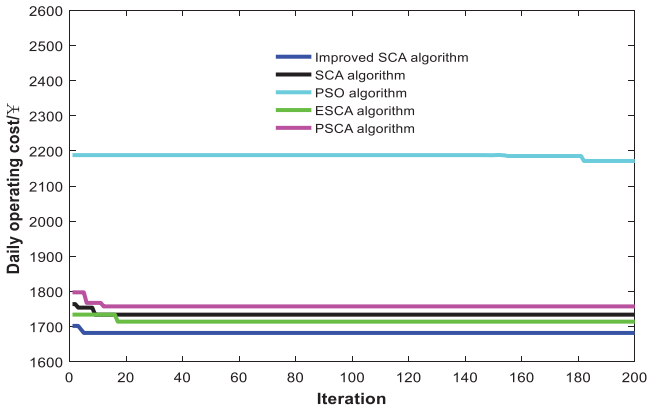

Figure 15: Comparison curve of the daily operating cost of ICEUS based on five algorithms on a typical day in summer

5 Conclusion

The structure of ICEUS was constructed in the study. The regulating characteristics of air conditioning and electric vehicles were discovered. The objective function was the lowest daily operating cost. The optimal dispatching model of ICEUS was established. The improved SCA solved the above model based on nonlinear factors and segment weight. The relevant conclusions are shown by example analysis as follows:

1) By regulating the electrical load, the peak-to-valley difference of the load was reduced. The kinds of energy supply and storage devices were optimally dispatched. The daily operating cost of ICEUS was effectively lowered. After electrical load regulation, the daily operating cost of ICEUS was cut by 1.3% and 1.5% in winter and summer, respectively. Moreover, in the peak period of the load, the rest of the electricity power was connected to the distribution network and supported the operation of the distribution network.
2) An improved SCA based on nonlinear factors and segmented weights is proposed to solve the optimal dispatching model of ICEUS. Compared with traditional algorithms, there are the advantages of fast convergence speed and high convergence accuracy in the improved SCA. The economic feasibility of the system operation was improved effectively. Therefore, the effectiveness and feasibility of the proposed algorithm in the study was proven.

In the next step, the model will be further improved. Joint optimal dispatching research on multiple ICEUS will be conducted. The rapid development of integrated energy technology will be promoted.

Acknowledgement: We appreciate the support from the School of Information Engineering at Inner Mongolia University of Science & Technology.

Funding Statement: The work is funded partly by the Natural Science Foundation of Inner Mongolia (2019MS05047), Key Technology Projects of Inner Mongolia Autonomous Region

(2019GG319) and Research on Key Technologies of MW advanced flywheel energy storage (2020ZD0017).

Conflicts of Interest: The authors declare that they have no conflicts of interest related to the present study.

References

1. Panagiotidou, M., Aye, L., Rismanchi, B. (2020). Solar driven water heating systems for medium-rise residential buildings in urban Mediterranean areas. *Renewable Energy, 147,* 556–569. DOI 10.1016/j.renene.2019.09.020.
2. Mendes, G., Ioakimidis, C., Ferrão, P. (2011). On the planning and analysis of integrated community energy systems: A review and survey of available tools. *Renewable & Sustainable Energy Reviews, 15,* 4836–4854. DOI 10.1016/j.rser.2011.07.067.
3. Koirala, B. P., Koliou, E., Friege, J., Hakvoort, R. A., Herder, P. M. (2016). Energetic communities for community energy: A review of key issues and trends shaping integrated community energy systems. *Renewable & Sustainable Energy Reviews, 56,* 722–744. DOI 10.1016/j.rser.2015.11.080.
4. Lin, W., Jin, X. L., Mu, Y. F., Jia, H. J., Xu, X. D. et al. (2018). A two-stage multi-objective scheduling method for integrated community energy system. *Applied Energy, 216,* 428–441. DOI 10.1016/j.apenergy.2018.01.007.
5. Wang, C. S., Lv, C. X., Li, P., Song, G. Y., Li, S. Q. et al. (2018). Modeling and optimal operation of community integrated energy systems: A case study from China. *Applied Energy, 230,* 1242–1254. DOI 10.1016/j.apenergy.2018.09.042.
6. Liu, D., Wu, J. Y., Lin, K. J., Wu, M. L. (2019). Planning of multi energy-type micro energy grid based on improved Kriging model. *IEEE Access, 7,* 14569–14580. DOI 10.1109/ACCESS.2019.2894469.
7. Qiao, X. B., Zou, Y., Li, Y., Chen, Y. Y., Liu, F. et al. (2019). Impact of uncertainty and correlation on operation of micro-integrated energy system. *International Journal of Electrical Power & Energy Systems, 112,* 262–271. DOI 10.1016/j.ijepes.2019.03.066.
8. Zhang, X., Zhang, M., Wang, W. Z., Yang, J. H., Jing, T. J. (2017). Rural micro energy grid optimization study based on improved crossbreeding particle swarm optimization algorithm. *Transactions of the Chinese Society of Agricultural Engineering, 33(11),* 157–164. DOI 10.11975/j.issn.1002-6819.2017.11.020.
9. Zhang, X., Yang, J. H., Wang, W. Z., Zhang, M., Jing, T. J. (2018). Integrated optimal dispatch of a rural micro-energy-gird with multi-energy stream based on model predictive control. *Energies, 11(12),* 3439–3461. DOI 10.3390/en11123439.
10. Askarzadeh, A. (2017). A memory-based genetic algorithm for optimization of power generation in a microgrid. *IEEE Transactions on Sustainable Energy, 9(3),* 1081–1089. DOI 10.1109/TSTE.2017.2765483.
11. Wu, D. H., Gao, C., Ji, Z. C. (2018). Economic optimization operation of the microgrid using the hybrid particle swarm optimization algorithm. *Control Theory & Applications, 35(4),* 457–467. DOI 10.7641/CTA.2017.70155.
12. Cinar, H., Kandemir, I. (2021). Active energy management based on meta-heuristic algorithms of fuel cell/battery/supercapacitor energy storage system for aircraft. *Aerospace, 8(3),* 85–105. DOI 10.3390/aerospace8030085.
13. Pang, W. T., Sheng, D. R., Chen, J. H., Li, W. (2020). Rolling strategy for multi unit coordinated operation with wind power system. *Acta Energiae Solaris Sinica, 41(11),* 234–240.
14. Tan, H., Yan, W., Wang, H. (2020). Optimal dispatch model of biogas-wind-solar isolated multi-energy mciro-grid based on thermal energy flow analysis of buildings. *Power System Technology, 44(7),* 2483–2492. DOI 10.13335/j.1000-3673.pst.2019.2434.

15. Zhang, X., Yang, J. H., Wang, W. Z., Jing, T. J., Zhang, M. (2018). Optimal operation analysis of the distribution network comprising a micro energy grid based on an improved grey wolf optimization algorithm. *Applied Sciences, 8(6),* 923–954. DOI 10.3390/app8060923.
16. Liu, J. F., Chen, J. L., Wang, X. S., Zeng, M., Huang, Q. Y. (2020). Energy management and optimization of multi-energy grid based on deep reinforcement learning. *Power System Technology, 44(10),* 3794–3803. DOI 10.13335/j.1000-3673.pst.2020.0144.
17. Hua, H. C., Qin, Y. C., Hao, C. T., Cao, J. W. (2019). Optimal energy management strategies for energy internet via deep reinforcement learning approach. *Applied Energy, 239,* 598–609. DOI 10.1016/j.apenergy.2019.01.145.
18. Hu, L. Y., Wang, L., Dong, M. F., Li, H. Z., Sun, K. et al. (2020). Energy consumption modeling and optimal operation analysis of regional integrated energy system based on improved petri net. *Electric Power Automation Equipment, 40(11),* 69–81. DOI 10.16081/j.epae.202010024.
19. Li, Y., Yang, Z., Li, G. Q., Zhao, D. B., Chen, C. (2019). Optimal scheduling of an isolated microgrid with battery storage considering load and renewable generation uncertainties. *IEEE Transactions on Industrial Electronics, 66(2),* 1565–1575. DOI 10.1109/TIE.2018.2840498.
20. Li, Y., Wang, C. L., Li, G. Q., Wang, J. L., Zhao, D. B. et al. (2020). Improving operational flexibility of integrated energy system with uncertain renewable generations considering thermal inertia of buildings. *Energy Conversion and Management, 207,* 112526–112540. DOI 10.1016/j.enconman.2020.112526.
21. Zhang, Z. D., Qiu, C. M., Zhang, D. X., Xu, S. W., He, X. (2019). A coordinated control method for hybrid energy storage system in microgrid based on deep reinforcement learning. *Power System Technology, 43(6),* 1914–1921. DOI 10.13335/j.1000-3673.pst.2018.2369.
22. Li, P., Wang, Z. X., Wang, J. H., Yang, W. H., Guo, T. Y. et al. (2021). Two-stage optimal operation of integrated energy system considering multiple uncertainties and integrated demand response. *Energy, 225,* 120256–12067. DOI 10.1016/j.energy.2021.120256.
23. Gao, X. S., Li, G. F., Xiao, Y., Bie, C. H. (2020). Day-ahead economical dispatch of electricity-gas-heat integrated energy system based on distributionally robust optimization. *Power System Technology, 44(6),* 2245–2254. DOI 10.13335/j.1000-3673.pst.2019.2356.
24. Li, P., Wang, Z. X., Wang, N., Yang, W. H., Li, M. Z. et al. (2021). Stochastic robust optimal operation of community integrated energy system based on integrated demand response. *International Journal of Electrical Power & Energy Systems, 128,* 106735–106745. DOI 10.1016/j.ijepes.2020.106735.
25. Liu, F., Bie, Z., Wang, X. (2019). Day-ahead dispatch of integrated electricity and natural gas system considering reserve scheduling and renewable uncertainties. *IEEE Transactions Sustainable Energy, 10(2),* 646–658. DOI 10.1109/TSTE.5165391.
26. Li, P., Wang, Z. X., Wang, J. H., Guo, T. H., Yin, Y. X. (2021). A multi-time-space scale optimal operation strategy for a distributed integrated energy system. *Applied Energy, 289,* 116698–116714. DOI 10.1016/j.apenergy.2021.116698.
27. Jiang, Y. C., Zeng, C. Y., Huan, J. J., Tan, Z. Y., Yu, M. Z. (2020). Multi-agent interest balance optimization scheduling of integrated energy based on improved NSGA-II. *Electric Power Automation Equipment, 40(7),* 17–25. DOI 10.16081/j.epae.202006024.
28. Wang, H. Y., Li, K., Zhang, C. H., Ma, X. (2020). Distributed coordinative optimal operation of community integrated energy system based on stackelberg game. *Proceedings of the CSEE, 40(17),* 5435–5444. DOI 10.13334/j.0258-8013.pcsee.200141.
29. Hou, R. (2019). Planning of reginal integrated energy system based on particle swarm optimization and its operation optimization. *Inner Mongolia Electric Power, 37(4),* 43–48. DOI 10.3969/j.issn.1008-6218.2019.04.003.
30. Mirjalili, S. (2016). SCA: A sine cosine algorithm for solving optimization problems. *Knowledge-Based Systems, 96,* 120–133. DOI 10.1016/j.knosys.2015.12.022.
31. Liu, Y., Ma, Y. (2017). Sine cosine algorithm with nolinear decreasing conversion parameter. *Computer Engineering and Applications, 53(2),* 1–5. DOI 10.3778/j.issn.10028331.1608-0349.

32. Gansu Provincial Development and Reform Commission (2020). Gansu province power grid sales price. https://xw.qq.com/amphtml/20201229A0IS2700.
33. Xian, X., Fan, C. G., Wen, S. S., Wang, Y. C., Chen, C. et al. (2016). Optimal deployment for island microgrid considering probabilistic factors of renewable energy generations. *Engineering Journal of Wuhan University, 49(1),* 101–104. DOI 10.14188/j.1671-8844.2016-01-017.
34. Pazouki, S., Haghifam, M. R., Moser, A. (2014). Uncertainty modeling in optimal operation of energy hub in presence of wind, storage and demand response. *International Journal of Electrical Power & Energy Systems, 61,* 335–345. DOI 10.1016/j.ijepes.2014.03.038.
35. Xu, Q. S., Zeng, X. D., Wang, K., Jiang, L. (2016). Day-ahead optimized economic dispatching for conbined cooling, heating and power in micro energy-grid based on hessian interior point method. *Power System Technology, 40(6),* 1657–1665. DOI 10.13335/j.1000-3673.pst.2016.06.008.
36. Zhang, Y. J., Lin, X. M., Xu, Z. H., Chen, Z. X. (2018). Dispatching method of micro-energy grid based on light robust optimization. *Automation Electric Power Systems, 42(14),* 75–82. DOI 10.7500/AEPS20171013005.
37. Lin, K. J., Wu, J. Y., Li, D., Li, D. Z., Gong, T. Z. (2019). Energy management optimization of micro energy grid based on hierarchical stackelberg game theory. *Power System Technology, 43(3),* 973–981. DOI 10.13335/j.1000-3673.pst.2018.1379.
38. Chen, N. B., Yang, M. Y. (2015). Research on optimal dispatch of a combined heat and power micro-grid system. *Modern Electric Power, 32(4),* 27–33. DOI 10.19725/j.cnki.1007-2322.2015.04.005.